Volume 4 | Number 29 | 7 August 2016 | Pages 4945–5070

Journal of Materials Chemistry B

Materials for biology and medicine

www.rsc.org/MaterialsB

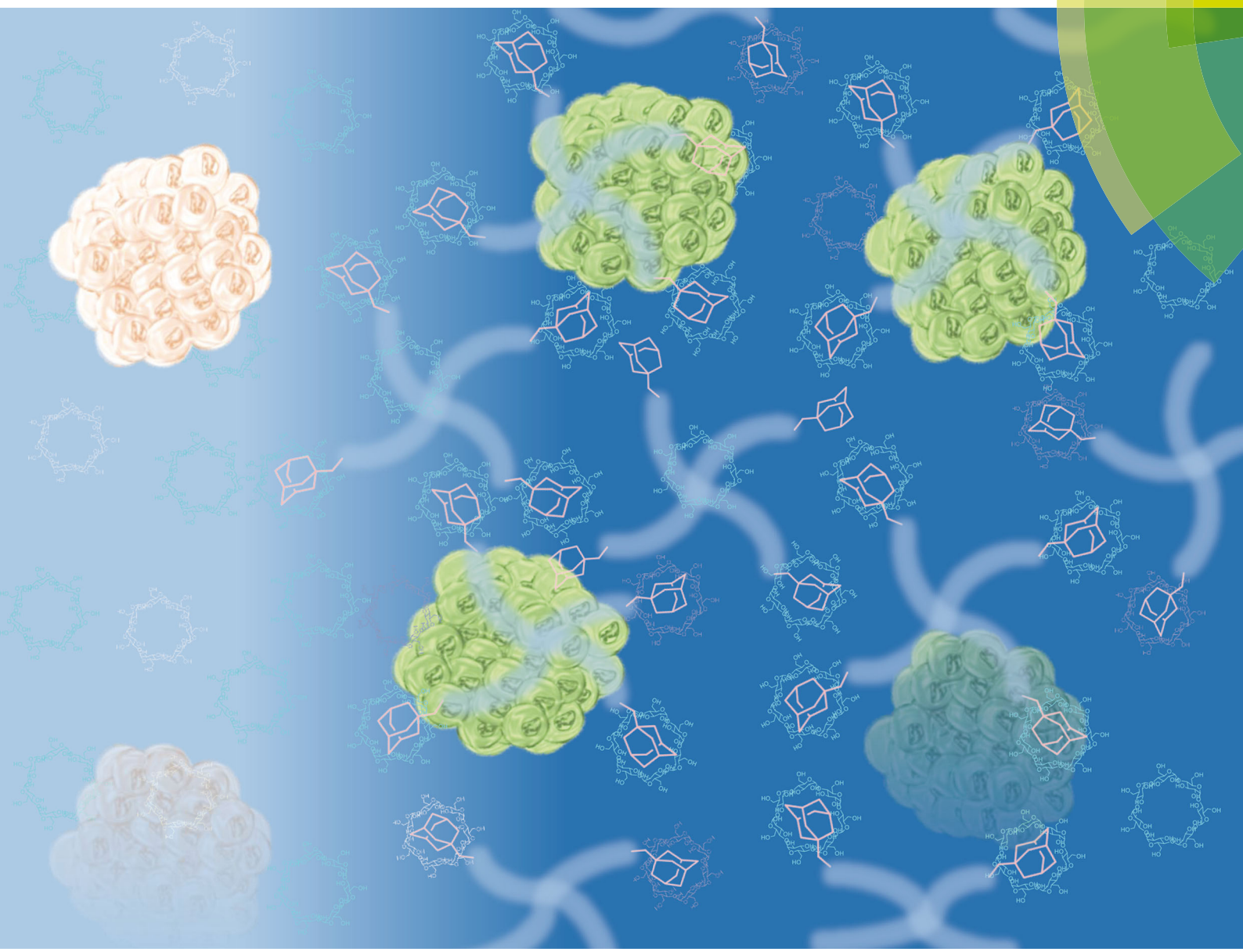

ISSN 2050-750X

ROYAL SOCIETY OF CHEMISTRY

COMMUNICATION

Han Shih and Chien-Chi Lin

Tuning stiffness of cell-laden hydrogel *via* host–guest interactions

175 YEARS

Journal of
Materials Chemistry B

COMMUNICATION

Tuning stiffness of cell-laden hydrogel *via* host–guest interactions†

Han Shih[a] and Chien-Chi Lin*[ab]

Cite this: *J. Mater. Chem. B*, 2016, 4, 4969

Received 11th April 2016,
Accepted 17th June 2016

DOI: 10.1039/c6tb00890a

www.rsc.org/MaterialsB

We report a dynamic hydrogel system with on-demand tunable matrix stiffness. The hydrogels are formed by thiol–allylether photo-click reaction using thiolated poly(vinyl alcohol) (TPVA), 4-arm poly(ethylene glycol)-allylether (PEG4AE), and mono-functional β-cyclodextrin-allylether (βCDAE). Adamantane-functionalized 4-arm PEG (PEG4AD) is used to stiffen hydrogels, whereas unmodified βCD is used to induce gel softening. The stiffening and softening processes are fully reversible and these hydrogels are ideal for investigating the effect of matrix mechanics on cell fate processes.

Dynamic cell-laden hydrogels are increasingly developed for studying the influence of matrix mechanics on cell fate processes.[1] For example, stiffness of a cell-laden hydrogel could be irreversibly decreased through user-controlled or cell-mediated matrix degradation.[2–5] On the other hand, the crosslinking density of some hydrogels could be increased irreversibly by applying secondary photo-crosslinking in the presence of the primary cell-laden hydrogel network.[6,7] One common feature of the aforementioned strategies is that the changes in matrix mechanics are irreversible, hence these matrices might not be ideal for studying the impact of dynamic matrix stiffening on cellular mechanobiology.[8,9] Here, we report a dynamic cell-laden hydrogel platform with post-gelation tunability in matrix stiffness, which is achieved by providing reversible host–guest interactions within the cell-laden hydrogel network. The hydrogels are prepared by a single step light-mediated thiol–allylether photo-click reaction using thiolated poly(vinyl alcohol) (TPVA), 4-arm poly(ethylene glycol)-allylether (PEG4AE), and β-cyclodextrin-allylether (βCDAE). The thiol–allylether photo-click gelation is compatible with *in situ* cell encapsulation and the stiffness of the hydrogel are tuned through non-covalent host–guest interactions between network-immobilized βCD and soluble 4-arm PEG-adamantane (PEG4AD) supplied on demand. The stiffening/softening processes are fully reversible by means of incubating gels in PEG4AD and βCD solutions, respectively. More importantly, the magnitude of the stiffness change can be tuned from several hundreds to a few kilo-Pascals, a range relevant to many cell fate processes.[10]

The influence of matrix biomechanical properties on cell fate has been intensively studied in the past decade.[8,11–15] In particular, the differentiation of mesenchymal stem cells (MSC) has been shown to depend on substrate stiffness.[10,11,16,17] Furthermore, mechanical properties of tissues have been implicated in invasion and drug resistance of cancer cells,[8,9,18–20] as well as in myofibroblastic activation of hepatic stellate cells and valvular interstitial cells.[21–24] It is commonly accepted that a cell culture matrix should present relevant mechanical properties for maintaining appropriate cell phenotype,[25,26] and the ultra-stiff tissue culture plastics (TCP) fail to provide such a physiologically relevant context. On the other hand, commercially available three-dimensional (3D) cell culture matrices are mechanically unstable and with limited tunability in stiffness post-gelation.[27] In view of the challenges facing these cell culture platforms, the past decade has witnessed increasing interests in 3D cell culture matrices with tailor-made and dynamically tunable biophysical and biochemical properties.[28,29] To affect cell fate processes in 3D, synthetic polymeric cell-laden hydrogels can be designed to undergo different modes of degradation, including hydrolytic, enzymatic, or photolytic degradation.[2–5] Hydrogels can also be hardened through secondary radical-mediated chain-growth or step-growth photopolymerizations.[6,7] For example, the presence of excess unreacted vinyl groups in the primary hydrogel network permits additional crosslinking reactions for network stiffening.[6,7] Although this approach readily increases hydrogel crosslinking density and stiffness, additional radicals formed during secondary photocrosslinking might be a confounding factor. While these dynamic material systems have demonstrated improvements over the conventional static cell culture systems, the stiffness of these hydrogels can only be decreased or increased irreversibly.

[a] *Weldon School of Biomedical Engineering, Purdue University, West Lafayette, IN, USA*

[b] *Department of Biomedical Engineering, Indiana University-Purdue University Indianapolis, Indianapolis, IN, USA. E-mail: lincc@iupui.edu*

† Electronic supplementary information (ESI) available: Synthesis protocol for PEGNB, PEG8aNB; methods for hydrogel fabrication, swelling, and mesh size calculations; additional results. See DOI: 10.1039/c6tb00890a

A hydrogel system with reversibly tunable matrix crosslinking and stiffness should be highly desirable in the study of cellular mechanobiology. An approach suitable for achieving reversible matrix crosslinking is the supramolecular host–guest interactions, which have been used extensively to enhance solubility of hydrophobic drugs and to design self-healing polymers.[30–32] For example, the hydrophobic cavity of macrocyclic molecules (*e.g.*, CD, and cucurbit[8]uril) can reversibly bind to a variety of hydrophobic drug molecules (*e.g.*, curcumin, paclitaxel, doxorubicin, *etc.*).[32–36] In another example, light-responsive supramolecular hydrogels formed from azobenzene-functionalized hyaluronan (Azo-HA) and CD-functionalized polymers were used to encapsulate proteins and cells when Azo is in *trans* conformation, which permits CD/Azo complexation and network formation.[37,38] Upon light exposure, Azo undergoes *trans*-to-*cis* isomerization, resulted in the disruption of CD/Azo complexes and the liberation of proteins and cells.[37,38] Supramolecular 'host–guest' interactions between adamantane (AD) and CD have also been exploited for forming cell-laden hydrogels exhibiting injectable and shear-thinning properties.[39–42] To the best of our knowledge, however, supramolecular chemistry and host–guest interactions have not been exploited to induce reversible post-gelation hydrogel stiffening and/or softening in the presence of cells.

Here, we report the design of cell-laden hydrogels with reversibly tunable stiffness by means of non-covalent and reversible host–guest interactions between pendant βCD and soluble PEG4AD. The primary hydrogel network was prepared from thiol–allylether photopolymerization (Fig. 1A) using TPVA (Fig. 1B) and PEG4AE (Fig. 1C) as the macromolecular crosslinkers. βCD-allylether (βCDAE, Fig. 1D) was co-polymerized in the primary hydrogel network as pendant 'host' motifs that can form additional physical crosslinks in the presence of soluble PEG4AD. Thiol–allylether photopolymerization was used to create the primary hydrogel network due to its orthogonal crosslinking, as well as its facile and quantitative immobilization of pendant βCD. Through supramolecular host–guest interactions, chemically immobilized 'host' molecules (*i.e.*, βCDAE, Fig. 1D, Fig. S1, ESI†) interact with user-supplied 'guest' macromolecules (*i.e.*, PEG4AD), resulting in increased hydrogel crosslinking density and elastic modulus. When needed, this 'stiffened' hydrogel can be 'softened' thermodynamically or through competitive binding provided by soluble βCDs. In principle, the process of hydrogel stiffening or softening can be repeated indefinitely if no other degradation mechanism exists.

To demonstrate the efficient crosslinking of orthogonal thiol–allylether hydrogels, we conducted *in situ* photorheometry using TPVA and PEG4AE in the absence (Fig. 1E) or presence of βCDAE (Fig. 1F). After the light was switched on, the thiol–allylether (TPVA-PEGAE) gelation occurred very rapidly (gel point: ~3 seconds) and the time required to reach 95% of ultimate stiffness was only ~2 minutes. The addition of βCDAE in the precursor solution led to a higher ultimate gel elastic modulus (G' ~ 2.4 kPa) and higher gel fraction (Fig. S2A, ESI†). One potential explanation for the higher initial gel stiffness in the presence of βCDAE (Fig. 1F) is that some βCDAE might have more than two allylether motifs that contribute to additional crosslinking (Fig. S1B, ESI†). Another

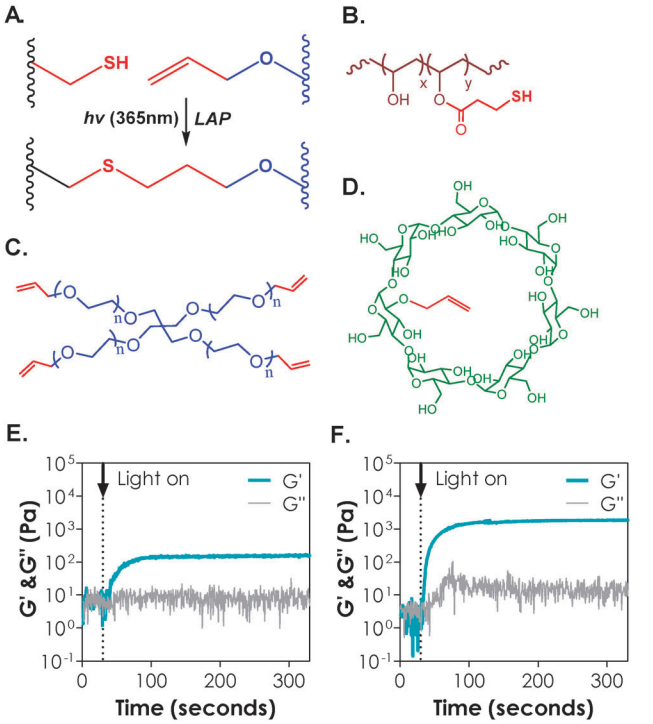

Fig. 1 (A) Schematics of thiol–allylether photo-click reaction using photoinitiator LAP and 365 nm light exposure (intensity: 10 mW cm^{-2}). (B–D) Chemical structures of the macromers used, including TPVA (B), PEG4AE (C), and βCDAE (D). (E and F) *In situ* photorheometry of thiol–allylether photopolymerization in the absence (E) or presence (F) of βCDAE (G': storage modulus; G'': loss modulus). [TPVA] = 2.5 wt% (total thiol from TPVA = 40 mM), [PEG4AE] = 0.8 mM (total allylether from PEG4AE = 3.2 mM, [βCDAE] = 27.6 mM). Light was turned on at 30 seconds (dotted line. N = 3, error bars were omitted for clarity).

potential is that immobilized bulky βCDAE decreased chain flexibility of linear TPVA, thereby increasing hydrogel stiffness. It is worth noting that, compared with similar light-mediated step-growth gelation using PEG-thiol and PEG-allylether, the gelation using TPVA and PEG4AE was faster and with the use of a significantly lower macromer contents (*i.e.*, 1.6 wt% of PEG4AE with 2.5 wt% TPVA).[43,44] This is likely due to the use of multi-functional TPVA (~10 thiol groups per molecule of $PVA_{6\,kDa}$). Overall, the use of efficient thiol–allylether photoclick reaction produces a stable βCD-immobilized hydrogel network for subsequent evaluation of hydrogel stiffening/softening using soluble PEG4AD macromers.

To ensure that βCDAE was successfully immobilized within the TPVA-PEG4AE hydrogel network, we prepared hydrogels using off-stoichiometric ratio of allylether to thiol (*i.e.*, $R_{[allylether]/[thiol]} = 0.8$). When compared with gelation using unmodified βCD, significantly lower free thiol was detected in the presence of βCDAE, indicative of βCDAE immobilization in the primary hydrogel network post-gelation (Fig. S2B, ESI†). ATR-FTIR characterization results also confirmed the immobilization of βCDAE in the thiol–allylether hydrogel network (1.5-fold and 34-fold increase in the areas under alcohol and carbonyl peaks, respectively. Fig. S2C, ESI†). We also conducted additional *in situ* photorheometry experiments to show that the gelation was indeed due to orthogonal

 This journal is © The Royal Society of Chemistry 2016

thiol–allylether reaction between TPVA and PEG4AE and not a result of homopolymerization of allylether-macromers (*i.e.*, βCDAE and PEG4AE, Fig. S3A, ESI†) or supramolecular 'threading' of βCDAE/TPVA or βCDAE/PEG4AE (Fig. S3B, ESI†). Another affirmation that βCD/PVA threading did not occur in this thiol–allylether gelation system (completing within 5 minutes) is that the threading events are typically achieved under extreme conditions such as high temperature (*e.g.*, 90 °C), high βCD concentration (*e.g.*, 70 wt%) or long incubation time (*e.g.*, 2–72 hours).[45–48]

We hypothesized that the reversible association and dissociation between network-immobilized βCD and soluble multi-functional PEG4AD (M_W: 10 kDa) macromer (Fig. 2A) could increase the crosslinking density, and hence elastic modulus, of this hydrogel.[32,49] We first investigated the tunability of hydrogel stiffness by incubating βCD-immobilized hydrogels in solution containing PEG4AD (Fig. 2B) at different concentrations. Since these thiol–allylether hydrogels were stiffened *via* host–guest supramolecular assembly, the amount of soluble PEG4AD supplemented to the βCD-immobilized hydrogels would affect the extent of host–guest interactions, and hence the degree of stiffening (Fig. 2C). As expected, hydrogel stiffness increased from 1.6- to 2-fold when the concentration of PEG4AD was increased from 2.5 wt% (*i.e.*, 10 mM AD) to 5 wt% (*i.e.*, 20 mM AD) (Fig. 2D). However, further increasing PEG4AD content to 10 wt% (*i.e.*, 40 mM AD) did not yield an even higher degree of stiffening because the concentration of AD at this condition exceeded the total βCD concentration (*i.e.*, 27.6 mM). As a result, additional PEG4AD became 'pendant' and did not contribute to the formation of additional crosslinking. We further evaluated the stiffening effect using TPVA-PEG4AE hydrogels with different initial gel stiffness. At a fixed TPVA content (2.5 wt%), increasing PEG4AE concentration yielded hydrogels with higher initial elastic modulus (Fig. 2E, 0.9 kPa to 4 kPa for 0.6 mM to 1.1 mM of PEG4AE, respectively). These hydrogels were separately stiffened using PEG4AD solution. Regardless of the starting equilibrium shear modulus, the stiffening process yielded hydrogels with significantly increased final elastic moduli (Fig. 2E, 2.3 kPa to 6.5 kPa). To evaluate the elastic nature of these hydrogels, we conducted frequency sweep oscillatory rheometry after incubating gels in the absence (Fig. S4A, ESI†) or presence (Fig. S4B, ESI†) of soluble PEG4AD. Results show that gel storage modulus (G') dominated loss modulus (G'') over the range of frequency tested, indicating the elastic property of the thiol–allylether hydrogels pre- and post-incubation with PEG4AD.

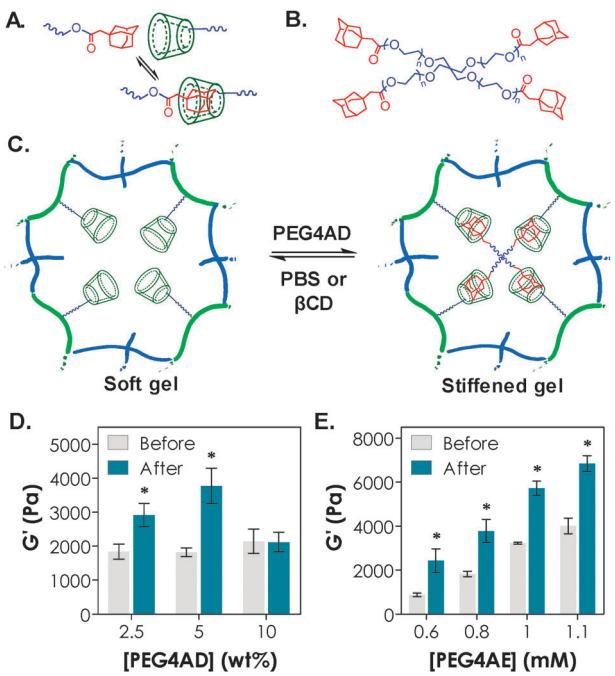

Fig. 2 (A) Schematic of a reversible βCD/AD complex. (B) Chemical structure of PEG4AD. (C) *In situ* stiffening of hydrogel through incubating βCD-containing gel in PEG4AD solution. Gel softening could be achieved by incubating the stiffened gel in PBS or solution containing unmodified βCD. (D) *In situ* stiffening using PEG4AD (10 kDa) at different concentrations. (E) Tuning the initial stiffness and dynamic stiffening of hydrogels through adjusting the content of PEG4AE in the pre-polymer solution. (Mean ± SD, $N = 3$, * indicates $p < 0.05$).

Although results so far show that the range of elastic moduli of hydrogels before and after PEG4AD-stiffening could be tuned in a physiologically relevant range (*i.e.*, elastic moduli ranging from 0.03 to 6 kPa),[10] it is necessary to determine the long-term stability of the *in situ* stiffened hydrogels. As shown in Fig. 3A, PEG4AD-induced gel stiffening (from ~2 to 3.5 kPa) could be maintained for more than one month as long as the βCD-immobilized hydrogels were incubated in PEG4AD-containing solution. After one month, the moduli of PEG4AD-stiffened gels started to decrease, which could be attributed to the hydrolysis of ester bonds in PEG4AD macromers (Fig. 2B). In a separate group where the stiffened hydrogels were transferred back to PBS following *in situ* stiffening, elastic moduli of the stiffened hydrogel decreased gradually (Fig. 3A, from 3.5 to 2.2 kPa in 48 days), most likely a result of the thermal relaxation of the host–guest interaction. Control experiments show that hydrogels incubated in either 4-arm PEG or PBS solution had minimal change in stiffness throughout the study, suggesting that the specificity of βCD/AD binding is essential in the stiffening of the hydrogels.

βCD/AD interactions are non-covalent, reversible, and can be disrupted through thermal relaxation or through a competitive kinetic binding process. We have demonstrated that PEG4AD-stiffened gels took weeks to soften when placed in PBS (Fig. 3A). This softening effect could be attributed to the dissociation and removal of PEG4AD from pendant βCD over time. Alternatively, a faster gel softening could be achieved by incubating the PEG4AD-stiffened hydrogels in solution containing unmodified βCD. Soluble βCD competes with PEG4AD for binding to immobilized βCD. As a result, the elastic moduli of PEG4AD-stiffened hydrogels incubated in βCD solution decreased from 3.1 to 2.3 kPa within 40 hours (Fig. 3B). When the *in situ* softened hydrogels were incubated in PEG4AD solution for another 40 hours, the hydrogels were stiffened again and the process of stiffening/softening was repeatable (Fig. 3B). For gels incubated in either PBS or 4-arm PEG/βCD, the stiffness remained steady throughout the study (Fig. 3B).

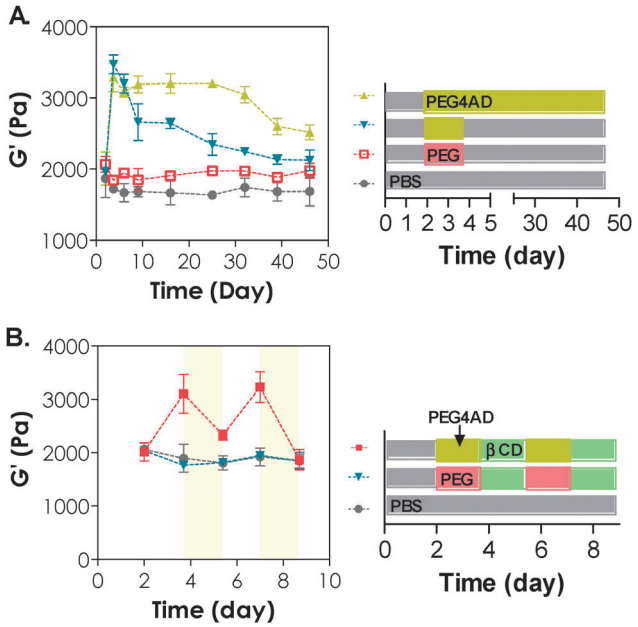

Fig. 3 (A) Effect of gel treatment conditions on the elastic moduli of thiol–allylether hydrogel. Right panel: timeline for the treatments of hydrogels. (B) Reversibly tuning the elastic moduli of thiol–allylether hydrogel. 5 wt% of PEG4AD (10 kDa) and 5 wt% of 4-arm PEG (10 kDa), respectively. Right panel: timeline for the treatments of hydrogels (2.5 wt% TPVA, 0.8 mM PEG4AE and 27.6 mM βCDAE, Mean ± SD, $N = 3$, * indicates $p < 0.05$).

Comparing to other hydrogels with stiffening or softening potential,[2–7] our dynamic thiol–allylether hydrogel offers a wider range of stiffness tunability (*i.e.*, from hundreds to thousands Pascals). For example, Rosales *et al.* prepared step-growth Michael-type hydrogels crosslinked with azobenzene-modified peptides that undergo *trans*-to-*cis* isomerization upon UV/visible light exposure.[50] The conformational change in azobenzene-containing peptide leads to changes in crosslinker length, and hence gel stiffness was controlled depending on light irradiation conditions. However, the magnitude of the elastic modulus change reported was about 100–200 Pa. Another difference between our approach and the light-responsive azobenzene-modified hydrogel or the secondary photo-crosslinking system was that the stiffening/softening of thiol–allylether hydrogels is a more gradual process (*i.e.*, hours in our system *vs.* minutes in previous stiffening processes) that should be more relevant to the time scale of most cell fate processes.[6]

To evaluate the cytocompatibility of this dynamic thiol–allylether hydrogel system, we performed *in situ* encapsulation of pancreatic MIN6 β-cells at a relatively low cell density (2×10^6 cells per mL). This cell density was used because a previous work has shown that MIN6 cells encapsulated in radical-mediated chain-growth photopolymerized PEG-diacrylate hydrogels did not survive well if the cell density was below 5×10^6 cells per mL.[51] We found that the step-growth thiol–allylether polymerization is highly cytocompatible for MIN6 β-cells as the encapsulated cells were viable regardless of the initial gel elastic modulus (0.6, 1.5 or 3.5 kPa, Fig. S5A, ESI†).[44,52] Furthermore, the encapsulated cells all formed multi-cell spheroids after 10 days of culture. While higher metabolic activity was detected in cells encapsulated in softer gel at day-10 post-encapsulation (Fig. S5B, ESI†), insulin mRNA level was lower in these cells (Fig. S5C, ESI†). Specifically, insulin expression was ~1.7-fold and 3.5-fold for soft and stiff gel, respectively (1-fold: insulin expression in cells encapsulated in 0.6 kPa gels). Another interesting phenomenon is that the sizes of cell spheroids formed within the stiffer hydrogels were noticeably smaller than those formed in the softer hydrogels, most likely because the stiffer hydrogels have higher crosslinking density that restricts the growth of the cell spheroids. The difference in cell spheroid sizes might be another confounding factor affecting insulin expression.

The higher insulin expression from cells encapsulated in stiffer hydrogel does not concord with a previous study conducted by Desai and colleagues, who cultured MIN6 β-cells using polymeric microwells with various moduli.[25] The conclusion from that study was that softer microwells promoted insulin expression in MIN6 β-cells and isolated islets. The discrepancy between current study and the reported results was likely due to the difference in cell-matrix interactions, because microwell does not provide uniform matrix contact for the cells. Furthermore, the function of β-cells in static thiol–allylether hydrogels might be affected by different amounts of radicals formed during cell encapsulation, different gel elastic moduli post-gelation, and/or different cell spheroids sizes.

Using the thiol–allylether dynamic hydrogel system, it is possible to study the influence of gel stiffness on cell fate without introducing additional radicals post cell encapsulation and without the confounding factor of cell spheroid sizes. Here, we encapsulated MIN6 β-cells in βCD-immobilized thiol–allylether hydrogels and cultured the cells for 5 days to allow the formation of multi-cell spheroids (Fig. 4A, condition ii). After *in situ* gel stiffening (Fig. S6, from 1.8 kPa to 2.5 kPa, ESI†), the viability of cells was evaluated using live/dead staining. Compared to cell-laden gels that did not undergo stiffening, cells encapsulated in PEG4AD stiffened gels had slightly more cell death as revealed by the confocal images of live/dead stained MIN6 β-cells (Fig. 4A). Quantitative ATP assay showed a reduction (not statistically significant) in total intracellular ATP when cell-laden hydrogels were subjected to PEG4AD (Fig. 4B, ~250 and 220 pmol of ATP/gel with and without exposure to PEG4AD, respectively). Since the concentration of PEG4AD selected was within the non-cytotoxic range (Fig. S7A, ESI†) and cells remained viable post-stiffening (Fig. 4A), it is highly plausible that the increased gel stiffness altered intracellular metabolism/signalling that led to a lower intracellular ATP content. More interestingly, MIN6 β-cells encapsulated in PEG4AD-stiffened gels had a 1.5-fold higher insulin mRNA level when compared with cells encapsulated in gels that did not undergo stiffening process (Fig. 4C). Results from control experiments show that PEG or PEG4AD did not induce up-regulation of insulin mRNA (Fig. S7B, ESI†). The effect of softening on cell fate was evaluated by incubating PEG4AD-stiffened gels in media containing βCD for 3 days (Fig. S6, ESI†). Compared to control gels that were not exposed to PEG4AD or βCD (Fig. 4A, condition iii), MIN6 cells encapsulated in hydrogel that underwent stiffening/softening had similar viability (Fig. 4A, condition iv) and ATP content (Fig. 4B), (180 pmol per gel). More importantly, there was a

 This journal is © The Royal Society of Chemistry 2016

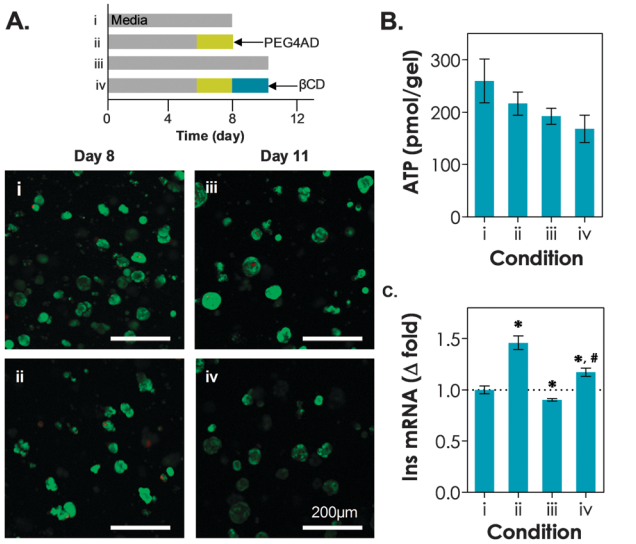

Fig. 4 Effect of PEG4AD stiffening and βCD softening on the cytocompatibility and functions of MIN6 β-cells. (A) Representative confocal z-stack images of MIN6 cells stained with live/dead staining kit on day 8 without or with PEG4AD stiffening (i & ii) and on day 11 without or with βCD softening (iii & iv). (B) ATP contents as assessed by CellTiter Glo® reagent. (C) Insulin mRNA expression was normalized to condition (i). All gel formulations contained 2.5 wt% TPVA, 0.8 mM PEG4AE and 27.6 mM βCDAE, 1 mM LAP, 2×10^6 cells per mL, and 365 nm light at 5 mW cm^{-2} (scales: 200 μm). Mean ± SD, $N = 3$, * or # indicate $p < 0.05$ compared to condition i and iii, respectively.

reduction in insulin mRNA expression after *in situ* softening (Fig. 4C, from 1.5 to 1.2-fold for condition (ii) and (iv), respectively), suggesting that the effect of matrix mechanics on insulin expression can be reversed upon softening of the hydrogel matrix.

Since the stiffening and softening of cell-laden thiol–allylether hydrogel did not introduce additional radicals and did not change the size of cell spheroids significantly, it is indicative that the insulin expression was affected in large part due to matrix stiffness. We hypothesize that the up-regulation of insulin in cells encapsulated in stiffened hydrogels was a collective result of altered cell–cell interactions,[53–55] hypoxia-related gene expression,[56,57] or stiffness-induced mechanotransduction in the cells. In the stiffened gels, tighter gel networks might constrain the encapsulated cells to make close contact with their neighboring cells. Furthermore, the stiffened matrix may alter other molecular targets downstream of mechanosensing pathways. While further investigations are required to elucidate the molecular mechanisms by which matrix stiffness affects mechanotransduction in cells encapsulated in this dynamic hydrogel, the current work demonstrates the concept and potential of using supramolecular host–guest interactions to tune matrix stiffness in cell-laden hydrogels.

Conclusions

In summary, we have synthesized a step-growth thiol–allylether photopolymerized hydrogel containing chemically immobilized βCD that complexes with soluble PEG4AD to form a dynamic hydrogel network with tunable stiffness. Thiol–allylether hydrogels crosslinked by TPVA, PEG4AE, and βCDAE exhibited rapid gelation kinetics and high tunability in crosslinking density. The process of gel stiffening/softening was repeatable by exposing gels in either PEGAD or βCD solutions, respectively. Most importantly, MIN6 β-cell fate is regulated in hydrogels that are stiffened *in situ*. Thiol–allylether hydrogel with immobilized βCD provided a wider range of stiffness tunability over existing dynamic hydrogels, and should be of great interest for studying the influence of biomechanical properties on cell fate processes.

Acknowledgements

This project was funded in part by the National Science Foundation CAREER award (#1452390), IUPUI Office of the Vice Chancellor for Research (OVCR) FORCES grant, Purdue Research Foundation Purdue Summer Faculty Research Grant, the Department of Biomedical Engineering at IUPUI Faculty start-up grant, and Purdue Research Foundation PhD Fellowship (to HS). The authors would like to thank Dr. Tsai-Yu Lin for his technical assistance with RNA isolation and gene expression work.

References

1 M. P. Lutolf and J. A. Hubbell, *Nat. Biotechnol.*, 2005, **23**, 47–55.
2 P. M. Kharkar, K. L. Kiick and A. M. Kloxin, *Chem. Soc. Rev.*, 2013, **42**, 7335–7372.
3 Y. Jiang, J. Chen, C. Deng, E. J. Suuronen and Z. Zhong, *Biomaterials*, 2014, **35**, 4969–4985.
4 H. Shih and C.-C. Lin, *Biomacromolecules*, 2012, **13**, 2003–2012.
5 A. M. Kloxin, M. W. Tibbitt, A. M. Kasko, J. A. Fairbairn and K. S. Anseth, *Adv. Mater.*, 2010, **22**, 61–66.
6 M. Guvendiren and J. A. Burdick, *Nat. Commun.*, 2012, **3**, 792.
7 K. M. Mabry, R. L. Lawrence and K. S. Anseth, *Biomaterials*, 2015, **49**, 47–56.
8 D. T. Butcher, T. Alliston and V. M. Weaver, *Nat. Rev. Cancer*, 2009, **9**, 108–122.
9 A. M. Handorf, Y. Zhou, M. A. Halanski and W.-J. Li, *Organogenesis*, 2015, **11**, 1–15.
10 A. J. Engler, S. Sen, H. L. Sweeney and D. E. Discher, *Cell*, 2006, **126**, 677–689.
11 N. Huebsch, P. R. Arany, A. S. Mao, D. Shvartsman, O. A. Ali, S. A. Bencherif, J. Rivera-Feliciano and D. J. Mooney, *Nat. Mater.*, 2010, **9**, 518–526.
12 M. Krieg, Y. Arboleda-Estudillo, P. H. Puech, J. Kafer, F. Graner, D. J. Muller and C. P. Heisenberg, *Nat. Cell Biol.*, 2008, **10**, 429–436.
13 J. D. Pajerowski, K. N. Dahl, F. L. Zhong, P. J. Sammak and D. E. Discher, *Proc. Natl. Acad. Sci. U. S. A.*, 2007, **104**, 15619–15624.
14 C. M. Kraning-Rush and C. A. Reinhart-King, *Cell Adhes. Migr.*, 2012, **6**, 274–279.
15 R. S. Stowers, S. C. Allen and L. J. Suggs, *Proc. Natl. Acad. Sci. U. S. A.*, 2015, **112**, 1953–1958.

16 J.-H. Seo, S. Kakinoki, T. Yamaoka and N. Yui, *Adv. Healthcare Mater.*, 2015, **4**, 215–222.
17 A. Singh, J. Zhan, Z. Ye and J. H. Elisseeff, *Adv. Funct. Mater.*, 2013, **23**, 575–582.
18 T. R. Cox and J. T. Erler, *Dis. Models & Mech.*, 2011, **4**, 165–178.
19 S. Sharma, C. Santiskulvong, J. Rao, J. K. Gimzewski and O. Dorigo, *Integr. Biol.*, 2014, **6**, 611–617.
20 C. Liu, Y. Liu, H.-g. Xie, S. Zhao, X.-x. Xu, L.-x. Fan, X. Guo, T. Lu, G.-W. Sun and X.-j. Ma, *Biotechnol. Appl. Biochem.*, 2015, **62**, 556–562.
21 M. Guvendiren, M. Perepelyuk, R. G. Wells and J. A. Burdick, *J. Mech. Behav. Biomed. Mater.*, 2014, **38**, 198–208.
22 H. Wang, M. W. Tibbitt, S. J. Langer, L. A. Leinwand and K. S. Anseth, *Proc. Natl. Acad. Sci. U. S. A.*, 2013, **110**, 19336–19341.
23 H. Wang, S. M. Haeger, A. M. Kloxin, L. A. Leinwand and K. S. Anseth, *PLoS One*, 2012, **7**, e39969.
24 A. M. Kloxin, J. A. Benton and K. S. Anseth, *Biomaterials*, 2010, **31**, 1–8.
25 C. E. Nyitray, M. G. Chavez and T. A. Desai, *Tissue Eng., Part A*, 2014, **20**, 1888–1895.
26 R. G. Wells, *Hepatology*, 2008, **47**, 1394–1400.
27 B. J. Gill, D. L. Gibbons, L. C. Roudsari, J. E. Saik, Z. H. Rizvi, J. D. Roybal, J. M. Kurie and J. L. West, *Cancer Res.*, 2012, **72**, 6013–6023.
28 C.-C. Lin, *RSC Adv.*, 2015, **5**, 39844–39853.
29 J. A. Burdick and W. L. Murphy, *Nat. Commun.*, 2012, **3**, 1269.
30 J. Hu, *Advances in Shape Memory Polymers*, Woodhead Publishing, 2013, pp. 111–127.
31 H. Meng and G. Li, *Polymer*, 2013, **54**, 2199–2221.
32 X. Ma and Y. Zhao, *Chem. Rev.*, 2015, **115**, 7794–7839.
33 B. W. Hwang, S. J. Kim, K. M. Park, H. Kim, J. Yeom, J.-A. Yang, H. Jeong, H. Jung, K. Kim, Y. C. Sung and S. K. Hahn, *J. Controlled Release*, 2015, **220**(Part A), 119–129.
34 M. Cheng, F. Shi, J. Li, Z. Lin, C. Jiang, M. Xiao, L. Zhang, W. Yang and T. Nishi, *Adv. Mater.*, 2014, **26**, 3009–3013.
35 E. A. Appel, F. Biedermann, U. Rauwald, S. T. Jones, J. M. Zayed and O. A. Scherman, *J. Am. Chem. Soc.*, 2010, **132**, 14251–14260.
36 E. A. Appel, R. A. Forster, M. J. Rowland and O. A. Scherman, *Biomaterials*, 2014, **35**, 9897–9903.
37 D. Wang, M. Wagner, H.-J. Butt and S. Wu, *Soft Matter*, 2015, **11**, 7656–7662.
38 L. Chen, X. Zhao, Y. Lin, Z. Su and Q. Wang, *Polym. Chem.*, 2014, **5**, 6754–6760.
39 F. van de Manakker, K. Braeckmans, N. e. Morabit, S. C. De Smedt, C. F. van Nostrum and W. E. Hennink, *Adv. Funct. Mater.*, 2009, **19**, 2992–3001.
40 C. B. Rodell, A. L. Kaminski and J. A. Burdick, *Biomacromolecules*, 2013, **14**, 4125–4134.
41 C. B. Rodell, J. W. MacArthur, S. M. Dorsey, R. J. Wade, L. L. Wang, Y. J. Woo and J. A. Burdick, *Adv. Funct. Mater.*, 2015, **25**, 636–644.
42 T. Kakuta, Y. Takashima and A. Harada, *Macromolecules*, 2013, **46**, 4575–4579.
43 L. A. Sawicki and A. M. Kloxin, *Biomater. Sci.*, 2014, **2**, 1612–1626.
44 H. Shih and C.-C. Lin, *Biomacromolecules*, 2015, **16**, 1915–1923.
45 W. Zhang, M. Chen and G. Diao, *Carbohydr. Polym.*, 2011, **86**, 1410–1416.
46 M. Constantin, G. Fundueanu, F. Bortolotti, R. Cortesi, P. Ascenzi and E. Menegatti, *Int. J. Pharm.*, 2004, **285**, 87–96.
47 J. L. Manasco, C. Tang, N. A. Burns, C. D. Saquing and S. A. Khan, *RSC Adv.*, 2014, **4**, 13274–13279.
48 S. Das, M. T. Joseph and D. Sarkar, *Langmuir*, 2013, **29**, 1818–1830.
49 C. B. Rodell, J. E. Mealy and J. A. Burdick, *Bioconjugate Chem.*, 2015, **26**, 2279–2289.
50 A. M. Rosales, K. M. Mabry, E. M. Nehls and K. S. Anseth, *Biomacromolecules*, 2015, **16**, 798–806.
51 C.-C. Lin and K. S. Anseth, *Proc. Natl. Acad. Sci. U. S. A.*, 2011, **108**, 6380–6385.
52 C.-C. Lin, A. Raza and H. Shih, *Biomaterials*, 2011, **32**, 9685–9695.
53 R. Jain and E. Lammert, *Diabetes, Obes. Metab.*, 2009, **11**(Suppl 4), 159–167.
54 A. Tomas, B. Yermen, L. Min, J. E. Pessin and P. A. Halban, *J. Cell Sci.*, 2006, **119**, 2156–2167.
55 D. C. Thurmond, C. Gonelle-Gispert, M. Furukawa, P. A. Halban and J. E. Pessin, *Mol. Endocrinol.*, 2003, **17**, 732–742.
56 L. Tillmar and N. Welsh, *Mol. Med.*, 2002, **8**, 263–272.
57 Y. Sato, H. Endo, H. Okuyama, T. Takeda, H. Iwahashi, A. Imagawa, K. Yamagata, I. Shimomura and M. Inoue, *J. Biol. Chem.*, 2011, **286**, 12524–12532.

 This journal is © The Royal Society of Chemistry 2016